Available online at www.sciencedirect.com
SCIENCE DIRECT®
Journal of Chromatography A, 1049 (2004) 25–36
JOURNAL OF CHROMATOGRAPHY A
www.elsevier.com/locate/chroma

Effect of the temperature on the isotherm parameters of phenol in reversed-phase liquid chromatography

Hyunjung Kim[a,b], Fabrice Gritti[a,b], Georges Guiochon[a,b,*]

[a] *Department of Chemistry, The University of Tennessee, Knoxville, TN 37996-1600, USA*
[b] *Division of Chemical Sciences, Oak Ridge National Laboratory, Oak Ridge, TN 37831-6120, USA*

Received 19 May 2004; received in revised form 10 August 2004; accepted 12 August 2004

Abstract

Adsorption isotherm data of phenol from an aqueous solution of methanol onto a C_{18}-bonded silica (Symmetry-C_{18}) were acquired by frontal analysis (FA) at six different temperatures, in a wide concentration range. The non-linear fitting of these data provided the bi-Langmuir model as best isotherm model, a conclusion further supported by the results of the calculation of the affinity energy distribution (AED). The isotherm parameters were obtained using several methods, the fitting of FA isotherm data, the calculation of the AED, and the inverse method, that uses overloaded elution band profiles. The different values obtained are in close agreement. They allow a quantitative investigation of the separate properties of the low- and the high-energy sites on the adsorbent surface. Increasing the temperature decreases the saturation capacity of the low-energy adsorption sites and the adsorption constant of the high-energy sites. In contrast, increasing the temperature does not cause any significant changes in either the saturation capacity of the high-energy sites or the adsorption constant of the low-energy sites.

Keywords: Adsorption isotherms; Affinity energy distribution; Inverse method; Band profiles; Phenol; Silica-based stationary phase

1. Introduction

Reversed-phase liquid chromatography (RPLC) has become the most popular method used to analyze and/or purify a variety of substances [1–3]. This popularity is explained by the development of manufacturing processes that reproducibly produce high quality particles of pure silica and bind it to alkyl chains. The resulting stationary phases provide high separation efficiency, convenience, versatility, and reproducibility. By modulating the retention of solutes with the aid of several external parameters, such as the mobile phase composition or the temperature, these stationary phases can be used to separate small or large molecules of widely different properties in clinical or environmental samples, in food or pharmaceutical products. In spite of this widespread usage of hydrophobic stationary phases, however, the retention mechanism in RPLC is still quite a controversial subject.

Two main models have been developed to explain the retention mechanism in RPLC, the solvophobic and the partition models [4,5]. The former attributes retention in RPLC to hydrophobic interactions taking place between the solutes and the mobile phase. In this model, the retention of solutes is a result of their relative lack of affinity for the mobile phase, which is expressed by their limited solubility. The role of the stationary phase on the retention in RPLC is considered as minor. In contrast, this role is considered as of major importance in the latter model, which assumes that retention is due to the adsorption of the solutes on the hydrophilic surface.

According to the partitioning model, there are two driving forces for the retention process. The first one is the difference in free energies of the solutes in the mobile and the stationary phases. The second one stems from the geometrical constrains of the alkyl bonded to the silica surface. These geometrically constrained alkyl chains may adopt different degrees of order, depending on the local bonding density of the stationary phase and on the nature of the mobile

* Corresponding author. Tel.: +1 865 974 0734; fax: +1 865 974 2667.
E-mail address: guiochon@utk.edu (G. Guiochon).

0021-9673/$ – see front matter © 2004 Elsevier B.V. All rights reserved.
doi:10.1016/j.chroma.2004.08.025

phase. As the chains become more ordered, the partition of the solutes between the bonded layer and the mobile phase becomes entropically less favorable. Many experimental results support the assumption that the properties of the bonded alkyl chains change depending on the composition of the mobile phase (e.g., the volume of the bonded layer) and that these changes affect the retention behavior of the solutes [6,7]. A more detailed understanding of the effect of the composition of the mobile phase on the properties of the alkyl chains was afforded by the measurement of the equilibrium isotherms of various solutes on RPLC stationary phases [8].

The temperature is another factor that influences the properties of the bonded alkyl chains. For example, the observation of non-linear Van't Hoff plots [9,10] and the characterization of C_{18}-silicas (Symmetry-C_{18}) by Raman spectroscopy [11,12] have been used to demonstrate that the stationary phase undergoes a phase transition from a "solid-like" ordered state to a "liquid-like" disordered state when the column temperature is increased. However, there is almost no data on the effect of temperature on the isotherm parameters, the saturation capacities and the adsorption constants of solutes on RPLC stationary phases. Only data on the effect of temperature on the retention factor of the solute (i.e., the initial slope of the isotherm) are available in the literature [13–15]. Acquiring isotherm parameters at different temperatures would allow a detailed investigation of the retention mechanisms involved.

In this study, we investigate the influence of the temperature on the equilibrium isotherm and on the overloaded band profiles of phenol on a C_{18}-silica. Previously, isotherm data of phenol were measured at room temperature on the same stationary phase, for a wide range of mobile phase composition. These data were best modeled with the bi-Langmuir isotherm model [16]. The systematic measurement of the isotherm data in a sufficiently wide temperature range allows the separate investigation of the influence of temperature on the parameters of the high- and the low-energy adsorption sites on the surface of the stationary phase. To determine the isotherm parameters of phenol at different temperatures, we employed several methods, the fitting of the frontal analysis data to an isotherm model, the calculation of the affinity energy distribution (AED), and the inverse method that derives the best values of the isotherm parameters from series of overloaded band profiles. The influence of the temperature on the isotherm parameters will be discussed in terms of the solubility of phenol and of the structure of the bonded alkyl chains.

2. Theory

2.1. Adsorption isotherm models

The Langmuir isotherm model is the simplest model used in studies of adsorption isotherm data. The Langmuir isotherm is written as:

$$q = \frac{q_s b C}{1 + bC} \tag{1}$$

where q_s is the monolayer saturation capacity and b is the adsorption constant of the studied compound. The Langmuir model assumes that the surface of the adsorbent is homogeneous, covered with only one type of adsorption sites, that these sites are localized, and that there are no interactions between adsorbate molecules. The adsorption energy of the adsorbent modeled by the Langmuir isotherm has a unimodal energy distribution, with an infinitely narrow mode.

The simplest extension of the Langmuir model to account for heterogeneous adsorption sites on the surface is the bi-Langmuir isotherm model (Eq. (2)), which assumes that the surface is composed of patches of two different types and independent adsorption sites. Its equation is written as:

$$q = \frac{q_{s1} b_1 C}{1 + b_1 C} + \frac{q_{s2} b_2 C}{1 + b_2 C} \tag{2}$$

where q_{s1} and q_{s2} are the saturation capacities for the first and the second type of sites, respectively, and b_1 and b_2 are the adsorption constants on the first and the second type of sites, respectively. Energy distributions based on the bi-Langmuir model display two peaks or modes, which are located at the average adsorption energy of the two types of sites. The width of these two modes is expected to be 0.

One of the other simple models suggested for adsorption on heterogeneous surfaces is the Langmuir–Freundlich equation:

$$q = \frac{q_s (bC)^n}{1 + (bC)^n} \tag{3}$$

where q_s is the saturation capacity, b the adsorption constant, and n is the heterogeneity parameter, smaller than unity. The heterogeneity parameter characterizes the degree of heterogeneity of the surface or of the distribution of adsorption sites. The closer to 1.0 the value of n, the more homogeneous the adsorbent surface. The adsorption energy modeled by the Langmuir–Freundlich equation has a Gaussian distribution [17–21], with a maximum energy related to the adsorption constant (b), and a width related to the degree of heterogeneity of the surface (n), i.e., the more heterogeneous the adsorption site distribution is, the broader the Gaussian peak is.

2.2. The expectation maximization (EM) method

The EM method allows the calculation of the adsorption energy distribution, hence the characterization of the surface heterogeneity [22–28]. The apparent, global, or overall adsorption isotherm is related to the local isotherm and to the distribution of adsorption constants by the following equation:

$$q(C) = \int f(\ln K)\theta(K, C)\mathrm{d}\ln K \tag{4}$$

where $q(C)$ is the global isotherm that is determined experimentally, C the equilibrium mobile phase concentration, $f(\ln K)$ the adsorption-constant distribution, K the adsorption constant, and $\theta(K, C)$ is the local adsorption isotherm, which is assumed to be the Langmuir isotherm in this study. In the EM method, Eq. (4) is discretized into the following equation:

$$q_{\text{cal}}(C_i) = \sum_{j=1}^{M} f(\ln K_j)\theta(K_j, C_i)\Delta(\ln K) \tag{5}$$

where C_i is the experimental value of the mobile phase concentration, $\ln K_j$ the logarithmic value of adsorption constant (K) spanned continuously across the discretized grid, $\Delta(\ln K)$ the constant spacing between $\ln K$ values in the discretized space, and M is the total number of grid points in the space. All values of $\ln K$ in the discretized grid are divided up using two input parameters, $K_{\min}$ and $K_{\max}$, and the number of points to be calculated for the distribution. The values of $K_{\min}$ and $K_{\max}$ are determined experimentally as the reciprocal of the largest ($C_{\max}$) and smallest mobile phase concentration ($C_{\min}$) used in the measurements, respectively:

$$K_{\min} = \frac{1}{C_{\max}} \quad \text{and} \quad K_{\max} = \frac{1}{C_{\min}} \tag{6}$$

The EM method consists in the numerical calculation of the distribution ($f(K_j)$) by successive approximations. An initial estimate of the distribution is required. For this purpose and in order to minimize the amount of information introduced in the calculation of the distribution, the following constant initial distribution was used.

$$f(\ln K_j) = \frac{q_{\text{high}} - q_{\text{low}}}{\ln K_{\max} - \ln K_{\min}} \tag{7}$$

where q_{high} and q_{low} are the highest and the lowest experimental values of the adsorbed amounts measured, respectively. In this study, (0, 0) was included as the initial data points (i.e., $q_{\text{low}} = 0$). Eq. (7) provides a constant distribution across the entire adsorption constant range as the initial estimate.

The EM method compares the ratio of an experimental value of q (q_{exp}) to a calculated value of q (q_{cal}) at each data point, providing a vector, which is used iteratively to correct an estimate of the isotherm. This vector is then convoluted with the local isotherm model to obtain a correction vector (β) for the distribution, as shown in the following equation:

$$\beta_j = \sum_{i=1}^{N} \frac{q_{\text{exp}}(C_i)}{q_{\text{cal}}(C_i)} \theta(K_j, C_i)\Delta(\ln K) \tag{8}$$

where N is the number of data points, and i and j are indices for the concentration and the adsorption constant, respectively. The distribution function is then corrected by multiplying $f(\ln K_j)$ by the factor given by Eq. (8) at each $\ln K_j$:

$$f(\ln K_j)^k = \beta(\ln K_j) f(\ln K_j)^{k-1} \tag{9}$$

where k is the iteration number and $f(\ln K_j)^{k-1}$ is the previous estimate of the distribution. The iteration continues by recalculating Eq. (5) with the new estimate (expectation) and correcting the distribution using Eqs. (8) and (9) (maximization).

2.3. The inverse method of isotherm determination (IM)

The inverse method is used to determine the adsorption parameters of an isotherm model from overloaded band profiles [29,30]. Obtaining the isotherm parameters using this method has practical advantages over the frequently used frontal analysis method because this method requires less time and lower amounts of chemicals. The IM method consists in the following steps. First, an isotherm model is selected and initial estimates for the adsorption parameters are made. Second, using this first isotherm estimate, the overloaded band profiles are calculated using a suitable chromatographic model. Third, the calculated overloaded band profiles are compared to the experimental band profiles by evaluating the following objective function:

$$\min \sum_i r_i^2 = \min \sum_i (C_i^{\text{sim}} - C_i^{\text{exp}})^2$$

where C_i^{sim} and C_i^{exp} are the calculated and the experimental concentrations at each data point. Finally, the parameters of the isotherm are changed in order to minimize the objective function, using an optimization routine.

To calculate the overloaded band profiles, the equilibrium-dispersive model of chromatography was used. This model assumes instant and constant equilibrium between the stationary and the mobile phase but a finite column efficiency originating from an apparent axial dispersion coefficient (D_{a}) that accounts the effects of axial dispersion and of the finite mass transfer across the column. The finite column efficiency and the apparent axial dispersion coefficient are related by the following equation that is valid under linear conditions.

$$D_{\text{a}} = \frac{uL}{2N}$$

where u is the mobile phase linear velocity, L the column length, and N is the column efficiency. The mass balance equation of the equilibrium-dispersive model for a single component is written as follows:

$$\frac{\partial C_i(z,t)}{\partial t} + F \cdot \frac{\partial q_i(z,t)}{\partial t} + u \cdot \frac{\partial C_i(z,t)}{\partial z} = D_{\text{a}} \cdot \frac{\partial^2 C_i(z,t)}{\partial z^2}$$

where C_i and q_i are the equilibrium concentrations of the component in the mobile and the stationary phase, respectively, z the length, t the time, and F is the phase ratio [$F = (1 - \varepsilon_{\text{t}})/\varepsilon_{\text{t}}$ where ε_{t} is the total porosity of the column]. The initial condition [C_i (z, 0)] and the boundary condition [C_i (0, t)] to solve the equation are written:

$$C_i(z, 0) = 0$$

$$C_i(0, t) = C_i^0, \quad 0 < t \le t_{\text{p}}$$

where t_p is the duration of the injection. The initial condition states that at $t = 0$ the column is equilibrated with the pure mobile phase while the boundary condition assumes that the sample is injected into the column as a rectangular pulse of length t_p. The mass balance equation was combined with the proper isotherm equation to calculate numerically the band profiles at the column outlet. This was accomplished by solving the integration using the Rouchon program based on the finite difference method.

3. Experimental

3.1. Chemicals and materials

The mobile phase used in this study was water–methanol (70:30, v/v), both liquids being HPLC-grade, purchased from Fisher Scientific (Fair Lawn, NJ, USA). The solution was filtered before use on an surfactant free cellulose acetate (SFCA) filter membrane, 0.2 μm pore size (Suwannee, GA, USA). The solutes used were phenol and thiourea, both purchased from Aldrich (Milwaukee, WI, USA). A manufacture-packed, 150 mm × 3.9 mm Symmetry (Waters, Milford, MA, USA) column [16,31] was used for this study. This column was packed with a C_{18}-bonded, endcapped, porous silica.

3.2. Determination of adsorption isotherms by frontal analysis (FA)

3.2.1. Liquid chromatography

The isotherm data were obtained by the frontal analysis method, using a Hewlett-Packard (Palo Alto, CA, USA) HP 1090 liquid chromatograph. This instrument is equipped with a multi-solvent system (tank volumes, 1 dm^3 each), an auto-sampler with a 250 μL sample loop, a diode-array UV detector, a column thermostat and a computer data acquisition station. The microcomputer of this system was used to program a series of breakthrough curves.

3.2.2. Experimental measurements of breakthrough curves

One of the pumps of the HPLC instrument was used to deliver a stream of pure mobile phase (methanol–water, 30:70, v/v), the other was used to deliver a stream of the pure sample solution at a constant flow rate of 1 mL/min. The concentration of the studied compound (phenol) in the stream percolating the column was determined by the concentration of the sample solution of phenol and the flow-rate fractions delivered by the two pumps. The concentration range of phenol studied was between 0.5 and 100 g/L. The FA experiments were carried out at six different temperatures (23, 35, 41, 53, 63, and 73 °C), with variations of the temperature during each series of experiments of ±1 °C. These are the actual values measured with a temperature probe located by the column, in its chamber, and are slightly different from those initially selected (25, 35, 45, 55, 65, and 75 °C). For each temperature, 33 consecutive breakthrough curves were recorded, with a sufficiently long delay time (15–25 min) between each breakthrough curve to allow the re-equilibrium of the column with the pure mobile phase. The injection time of the sample was fixed at 5 min for all FA experiments, so that, at the end of each experiment, the composition of the eluate was the same as that of the plateau injected at the column inlet. The detector signal was recorded at 292 nm to avoid recording any UV-absorbance signal above 1500 mAU.

The hold-up time was measured by using the auto sampler to inject a small amount of thiourea dissolved in the mobile phase (methanol–water, 30:70) into the column at each of the different temperatures studied. The extra column time corresponds to the migration time of the step front through the tubing between the pump and the column inlet. This time was measured as the hold-up time when a small dead volume union was used instead of the Symmetry column to connect injector and detector. The corresponding hold-up volume was 0.058 or 0.9 mL, depending whether it was measured from the auto sampler or from the pump system. The experimental data were corrected by subtracting the extra column volume.

3.2.3. Calculation of the isotherm data points

The amount of phenol adsorbed onto the stationary phase q^* at equilibrium with a given mobile phase concentration, C, was calculated using the equation:

$$q = \frac{C(V_{equ} - V_0)}{V_a} \tag{10}$$

where V_{equ} is the elution volume of the equivalent area of the solute, V_0 the dead volume, and V_a is the volume of the stationary phase. The value of V_{equ} for each breakthrough curve was calculated at the volume corresponding to the maximum numerical value of the first derivative of the breakthrough curve (inflection point). The value of V_a was calculated by subtracting V_0 from the geometrical volume of the column.

3.2.4. Fitting of the isotherm data to isotherm models

Non-linear regression of the experimental data to adsorption isotherm models was performed using Origin 6.0 (Northampton, MA, USA). The experimental data were fit to each isotherm model with weights ($1/q^2$) designed to put an even emphasis on each data point during the fitting process. The best isotherm parameters were selected by minimizing the residual sum of squares (RSS) for each isotherm model. To avoid being trapped in a local minimum in the regression process and to determine whether the solution converges toward a global minimum, several calculations were carried out, using different initial values of the parameters [32].

The different adsorption isotherm models were compared using the Fisher test (equation below). The best model se-

lected for the experimental data is the one, which gives the highest value of the Fisher parameter [32].

$$F_{\text{cal}} = \frac{(n-l)\sum_{i=1}^{n}(q_{\text{ex},i} - \overline{q_{\text{ex}}})^2}{(n-1)\sum_{i=1}^{n}(q_{\text{ex},i} - q_{t,i})^2} \quad (11)$$

where $\overline{q_{\text{ex}}}$ is the mean value of the experimental data q_{ex}, l the number of adjusted parameters of the model, and n is the number of data points.

The adsorption isotherm models used to fit the experimental isotherm data were the Langmuir, the bi-Langmuir, and the Langmuir–Freundlich isotherm models.

3.2.5. Calculation of the affinity distribution using the expectation maximization method

The EM algorithm programmed in Fortran (Lahey/Fujitsu Fortran 95, Incline Village, NV, USA) was used to calculate the affinity energy distributions. One hundred grid points in the K-space were used to logarithmically digitize the range between K_{min} = 0.0001 L/g and K_{max} = 2 L/g. The algorithm performed 1×10^7 iterations. The calculated AED from this algorithm shows the differential saturation at each point $[q_s(K_j)]$ as a function of $\log_{10} K_j$, where $q_s(K_j) = f(\ln K_j)\ \Delta(\ln K)$. To estimate the isotherm parameters from the calculated AED, the values of q_s comprising one peak were added to obtain the saturation capacity of the corresponding type of sites, and the value of $\ln K_j$ for the peak was used to calculate the adsorption constant of the corresponding site.

3.2.6. Measurement of the overloaded band profiles

Overloaded band profiles of phenol on Symmetry-C_{18} were recorded at each temperature, independently from the FA measurements. The injections of phenol were done with the pump, at three different concentrations, 10, 50, and 100 g/L. The band profiles were recorded at 292 nm. The detector response was calibrated from the UV-absorbance value measured on the plateau following each breakthrough curve and the absorbance units (mAU) were converted to concentration units (g/L). A third order polynomial was used as a calibration function for all experimental data.

The inverse method was used to derive the best values of the isotherm parameters from overloaded band profiles. To use this method, an isotherm model and initial adsorption parameters are needed. Three band profiles were recorded at 23 °C, with injections of phenol at the three different concentrations (see above), for 40 s, shortly after acquisition of the frontal analysis data of phenol at 23 °C. For the calculated band profiles, the bi-Langmuir model was selected as the isotherm model, and the initial estimates for the adsorption parameters were the values obtained by fitting the frontal analysis data at 23 °C to the bi-Langmuir isotherm model. These parameters were further optimized to minimize the difference between the experimental and the calculated band profiles. These optimized bi-Langmuir isotherm parameters at 23 °C were used as initial estimates to calculate the isotherm parameters at the different temperatures by the inverse method.

4. Results and discussion

The goal of this study was to determine how the isotherm parameters of phenol on Symmetry-C_{18} change with increasing temperature. For that purpose, three independent methods were employed to obtain the isotherm parameters. These methods were the non-linear fitting of the FA experimental isotherm data to the bi-Langmuir isotherm model; the calculation of the affinity energy distribution from the raw isotherm data; and the inverse method, from overloaded band profiles. Using the isotherm parameters obtained from each of these methods, we studied the effects of the temperature on the isotherm parameters of phenol on Symmetry-C_{18}.

4.1. Determination of the bi-Langmuir isotherm parameters

4.1.1. Frontal analysis and non-linear fitting to bi-Langmuir isotherm model

As a first step, isotherm data of phenol were acquired by frontal analysis at each temperature. Fig. 1 shows these data (symbols) and their best fits to the bi-Langmuir isotherm model (solid lines) at each temperature. In agreement with previous results [16], the highest value of the Fisher parameter (16,000) and the lowest value of the residual sum of squares (3.3) were obtained when the adsorption data at 23 °C were fitted to the bi-Langmuir model. Fits to the Langmuir or the Langmuir–Freundlich isotherm model gave poor results (Table 1). The same statistical tests showed that the

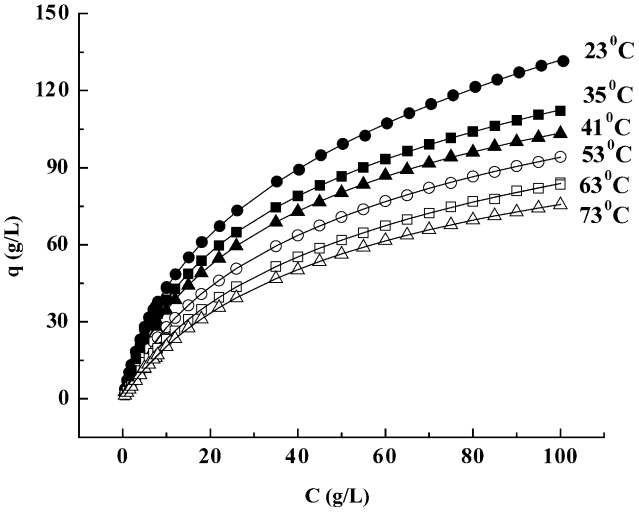

Fig. 1. Adsorption equilibrium of phenol onto Symmetry-C_{18} from methanol–water (30:70, v/v) at six different temperatures. Symbols: experimental isotherm data. Lines: best fits of the experimental data to the bi-Langmuir isotherm model.

Table 1
Fisher parameters (F_{cal}) and residual sum of squares (RSS) calculated from fitting the experimental isotherm data to each isotherm model at each temperature

Temperature (°C)	Isotherm model					
	Langmuir		Bi-Langmuir		Langmuir–Freundlich	
	RSS	F_{cal}	RSS	F_{cal}	RSS	F_{cal}
23	786	70	3.3	16000	168	300
35	274	500	2.7	30000	44	3000
41	217	200	2.9	11000	47	700
53	50	600	5.1	6000	30	900
63	157	300	2.2	12000	57	800
73	25	3000	0.5	12000	9.5	6000

bi-Langmuir model is the model that accounts best for the adsorption of phenol at each temperature, as indicated by the highest Fisher parameter and the lowest residuals, compared to the other isotherm models (see Table 1). Therefore, the bi-Langmuir parameters were used to investigate the influence of the temperature on the isotherm parameters of phenol.

In addition to showing good agreement with the bi-Langmuir isotherm model, the data in Fig. 1 show that the amount of phenol adsorbed at each mobile phase concentration decreases with increasing temperature and that the isotherm parameters are strong functions of temperature. The set of bi-Langmuir isotherm parameters obtained by isotherm fitting at the different temperatures is summarized in Table 2. The influence of the temperature on each parameter obtained with the three different methods used is discussed in more detail in a later section.

4.1.2. Estimation from affinity energy distribution

The expectation maximization algorithm was used to calculate the affinity energy distribution from the raw adsorption data, without requiring any prior assumption on the isotherm model [23–28]. The AED derived from the EM method were used to validate the isotherm model selected from the fitting process. Fig. 2 shows the AED calculated by EM from the isotherm data at each temperature. The AEDs at the different temperatures were calculated using the same range of adsorption constants (b), between 0.0001 and 2 L/g, and the same number of iterations (10^7 iterations). These AEDs exhibit two well-resolved peaks at low and high energy, at each temperature (Fig. 2). This further supports the choice of the bi-Langmuir isotherm model to account for the adsorption of phenol on Symmetry-C_{18} at all temperatures.

Fig. 2 shows also that the adsorption energy on the high-energy sites tends toward the adsorption energy on the low-energy sites with increasing temperature, although no systematic change of the energy of the low-energy modes can be observed with increasing temperature. In the same time, the height of the low-energy modes decreases while there are no significant changes in the height of the high-energy modes. These qualitative assessments of the AEDs at the different temperatures indicate that temperature has a significant influence on the adsorption energy on the high-energy sites and on the saturation capacity of the low-energy sites. The bi-Langmuir parameters were estimated from the AED (data in Table 3) at each temperature. The comparison with the parameters obtained from the other methods will be discussed later.

4.1.3. The inverse method and the overloaded band profiles

Fig. 3 shows the band profiles recorded at six different temperatures upon the injection of a solution at 10 g/L phenol for 40 s. For the sake of simplicity, the band profiles obtained with higher concentrations of phenol (i.e., 50 and 100 g/L) are not shown. The same trend was observed, regardless of the concentration of phenol injected. Qualitatively, Fig. 3 shows that the shock layer of the overloaded band appears earlier when temperature increases, in agreement with a decreasing retention time of phenol. Also, the tails of the profiles decay faster with increasing temperature. These results illustrate qualitatively the variations of the parameters of the adsorption isotherm of phenol with temperature.

In order to determine the values of the adsorption-isotherm parameters from the band profiles at the different temperatures, the inverse method was employed. The three band profiles obtained with 10, 50, and 100 g/L solutions were simultaneously used in the calculations of the isotherm. The bi-Langmuir isotherm model was used for these calcula-

Table 2
Best bi-Langmuir isotherm parameters of phenol on Symmetry-C_{18} at six different temperatures using a methanol–water (3:7, v/v) as a mobile phase

Temperature (°C)	Bi-Langmuir parameters			
	q_{s1} (g/L)	b_1 (L/g)	q_{s2} (g/L)	b_2 (L/g)
23	189.92	0.0066	61.49	0.105
35	134.37	0.0067	65.32	0.085
41	112.90	0.0096	54.29	0.084
53	111.82	0.0073	55.35	0.057
63	119.22	0.0049	53.57	0.049
73	84.93	0.0043	64.42	0.036

The best bi-Langmuir isotherm parameters were obtained by fitting the experimental adsorption data obtained by FA to the bi-Langmuir isotherm model.

Table 3
Best bi-Langmuir isotherm parameters of phenol on Symmetry-C_{18} at six different temperatures using a methanol–water (3:7, v/v) as a mobile phase

Temperature (°C)	Bi-Langmuir parameters			
	q_{s1} (g/L)	b_1 (L/g)	q_{s2} (g/L)	b_2 (L/g)
23	199	0.005	64.6	0.1060
35	134	0.007	64.2	0.0828
41	113	0.010	53.2	0.0828
53	115	0.006	58.1	0.0572
63	121	0.007	43.9	0.0572
73	84	0.008	46.5	0.0447

The best bi-Langmuir isotherm parameters were estimated from affinity energy distribution calculated from the raw adsorption data using the expectation maximization algorithm.

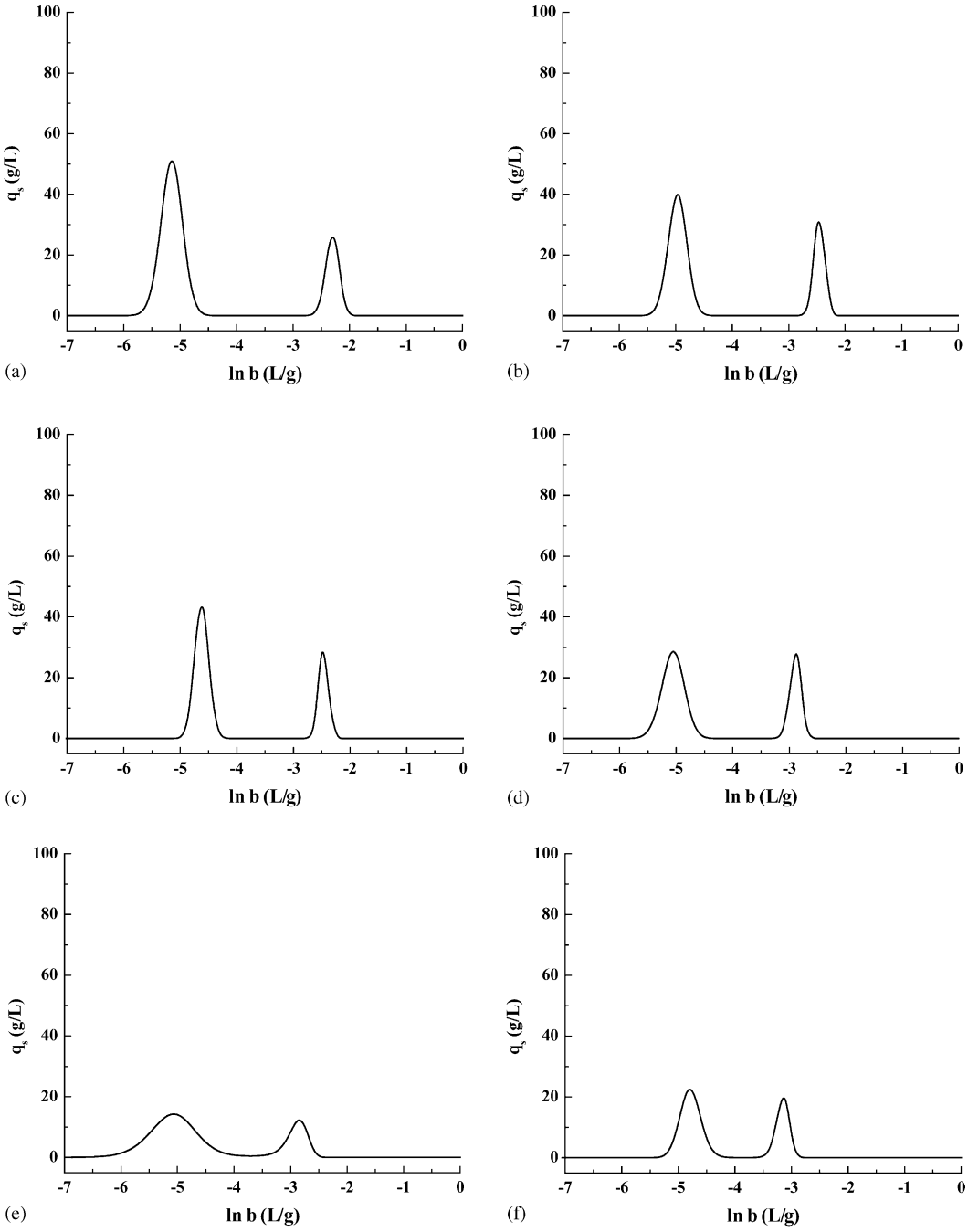

Fig. 2. Affinity energy distribution of phenol on Symmetry-C_{18}. Temperatures: (a) 23 °C, (b) 35 °C, (c) 41 °C, (d) 53 °C, (e) 63 °C, and (e) 73 °C. The affinity distribution was calculated by expectation maximization algorithm from the raw experimental isotherm data of phenol. One hundred grid points in K-space were used to logarithmically digitize the range between K_{min} = 0.0001 L/g and K_{max} = 2 L/g.

tions. The calculations were performed with the values of the isotherm parameters obtained at 23 °C as the initial estimates of the adsorption parameters. Fig. 4 compares the experimental (dotted lines) and the calculated band profiles derived from the inverse method (solid lines) at each temperature, using only the profiles recorded with injection concentrations of 10 g/L for 40 s as the example. As shown in Fig. 4, there is a very good agreement between the experimental and the calculated band profiles. The values of the bi-Langmuir isotherm parameters obtained at each temperature using the profiles obtained with the three different phenol concentrations are summarized in Table 4.

4.2. Influence of the temperature on the bi-Langmuir parameters

The values of the bi-Langmuir isotherm parameters of phenol at six different temperatures, estimated from the three

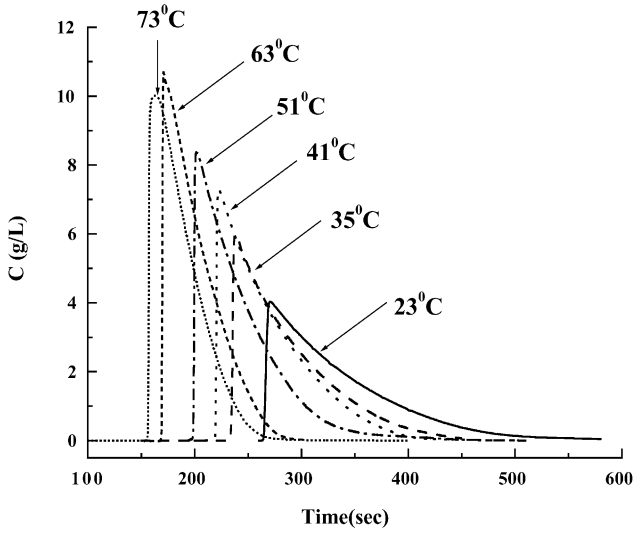

Fig. 3. Evolution of the overloaded band profiles of phenol (injection of a 10 g/L solution for 40 s) with increasing temperature. Same experimental conditions as in Fig. 1.

independent approaches used are reported in Tables 2–4 and plotted in Fig. 5. In Table 4 and Fig. 5, the values of the adsorption constant (b_1) and the saturation capacity (q_{s1}) of the low-energy sites obtained with the inverse method and by injecting 10 g/L solutions of phenol were omitted. The reason is that, at this relatively low phenol concentration, the high-energy sites are not fully populated, the occupation density of the low-energy sites is quite low, and the isotherm parameters of the low-energy sites cannot be accurately estimated. A few general trends can be observed in Fig. 5 for the different bi-Langmuir parameters, regardless of the method used to estimate them. (1) The saturation capacity of the low-energy sites (q_{s1} in Fig. 5a) decreases with increasing temperature. (2) The adsorption constant of the low-energy sites (b_1 in Fig. 5b) seems to be almost independent of the temperature even though there is slight tendency to increase with increasing temperature, except for the sets of parameters obtained from the AED calculations that are not conclusive. (3) The saturation capacity of the high-energy sites (q_{s2} in Fig. 5c) is independent of the temperature. (4) The adsorption constant of the high-energy sites (b_2 in Fig. 5d) decreases rapidly with increasing temperature. Note that all three methods show that the equilibrium constant b_2 varies much faster with the temperature than the constant b_1.

The temperature dependence of the retention factors of many solutes on alkyl-bonded silica is well documented in the literature. Almost always, increasing the temperature decreases the retention factor [9,10]. However, the retention factor at infinite dilution shows only the combined effect of the influence of temperature on the low- and the high-energy sites, as explained in the following equation:

$$k'_0 = F\left(\frac{dq}{dC}\right)_{c=0} = F(b_1 q_{s1} + b_2 q_{s2}) \quad (12)$$

Even though the dependence of these four parameters on the temperature is widely different, as will be discussed later, studying the temperature dependence of k'_0 does not inform much on the retention mechanism. Thus, obtaining separately the four isotherm parameters, on the low- and the high-energy sites provides far greater insights into retention mechanisms and the role played by temperature.

From Eq. (12), we can separate the influences of the temperature on the contributions of the low- and the high-energy sites on the retention factor. By increasing the temperature from 23 to 73 °C, the contribution of the low-energy sites ($b_1 q_1$) decreases from 1.25 to 0.37, i.e., by 70% while the contribution of the high-energy sites ($b_2 q_2$) decreases from 6.47 to 2.31, i.e., by 63%. This result is consistent with the two third decrease of the retention factor and shows that the low- and the high-energy sites contribute in the same proportions to the decrease of the retention factor when the temperature increases. However, for the low-energy sites, it is a large decrease of the saturation capacity (q_{s1}) that is responsible for their decreased contribution to the retention factor. In contrast, for the high-energy sites, it is a large decrease in the adsorption constant (b_2) that is responsible for their decreased contribution to the retention factor.

The retention model, which is widely accepted in the literature, suggests that increasing the temperature affects the

Table 4
Best bi-Langmuir isotherm parameters of phenol on Symmetry-C_{18} at six different temperatures using a methanol–water (3:7, v/v) as a mobile phase

Temperature (°C)	Bi-Langmuir isotherm parameters											
	10 g/L				50 g/L				100 g/L			
	q_{s1} (g/L)	b_1 (L/g)	q_{s2} (g/L)	b_2 (L/g)	q_{s1} (g/L)	b_1 (L/g)	q_{s2} (g/L)	b_2 (L/g)	q_{s1} (g/L)	b_1 (L/g)	q_{s2} (g/L)	b_2 (L/g)
23	n.a[a]	n.a	49.8	0.1469	148.8	0.0072	62.1	0.1041	128.7	0.0099	63.6	0.1017
35	n.a	n.a	50.4	0.1140	127.3	0.0071	66.7	0.0831	93.5	0.0109	66.9	0.0965
41	n.a	n.a	51.1	0.0937	104.2	0.0074	67.4	0.0823	67.7	0.0117	71.6	0.0788
53	n.a	n.a	52.6	0.0763	92.4	0.0072	64.2	0.0668	79.6	0.0117	66.9	0.0749
63	n.a	n.a	51.2	0.0593	53.6	0.0085	67.4	0.0495	47.3	0.0129	65.1	0.0618
73	n.a	n.a	53.4	0.0478	28.8	0.0119	77.5	0.0304	42.8	0.0138	64.3	0.0402

The inverse method was used to obtain the best bi-Langmuir isotherm parameters from the three band profiles obtained by injecting 10, 50, and 100 g/L of phenol for 40 s.

[a] Non-available data due to the large errors on estimating isotherm parameters of the low-energy sites from overloaded band profiles obtained by injecting low concentration of phenol.

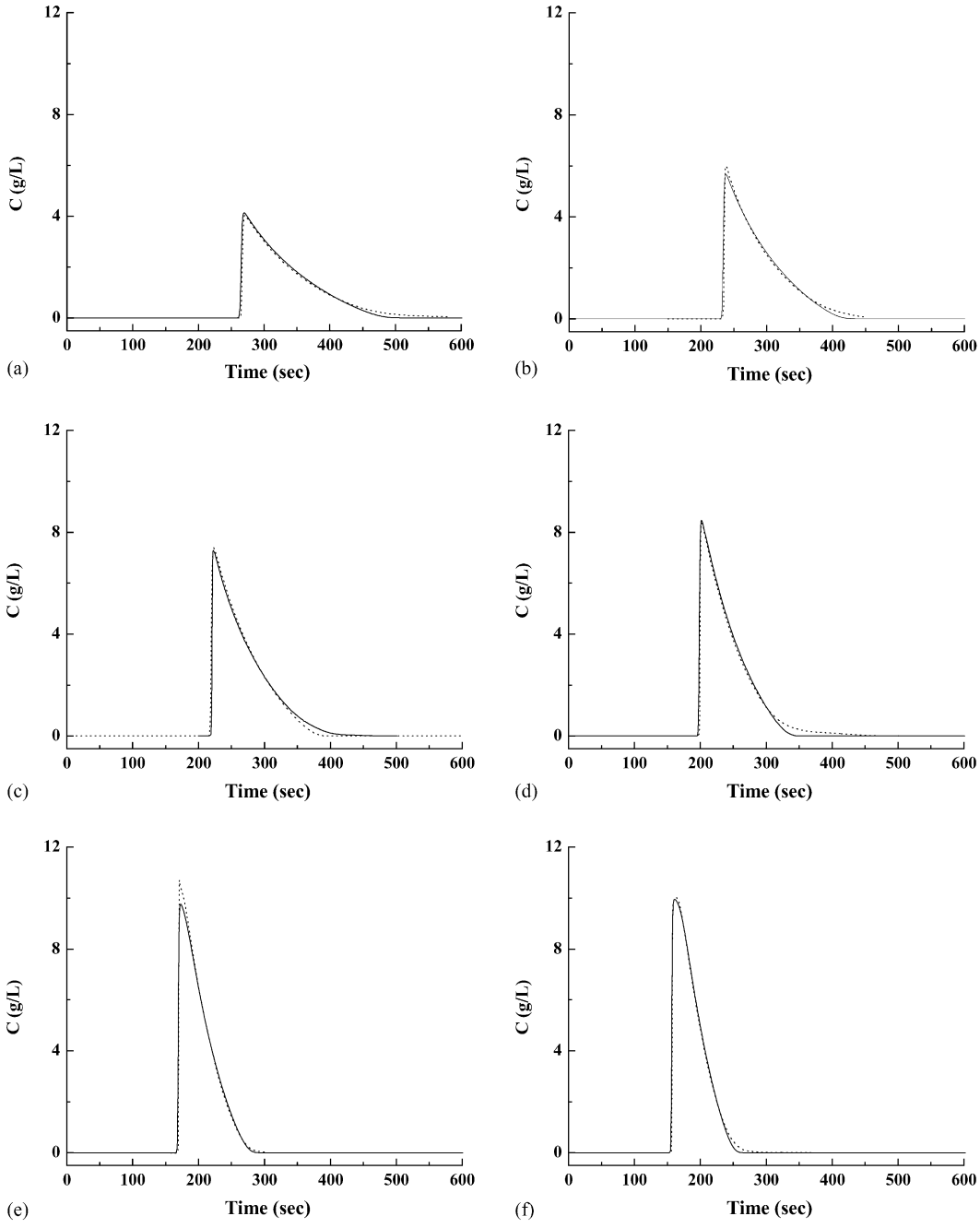

Fig. 4. Experimental (dotted lines) and calculated (solid lines) band profiles of phenol (injection of a 10 g/L solution for 40 s). Temperatures: (a) 23 °C, (b) 35 °C, (c) 41 °C, (d) 51 °C, (e) 63 °C, and (f) 73 °C. Same experimental conditions as in Fig. 1.

isotherm parameters of phenol in two ways [3,4]. First, increasing the temperature increases the solubility of phenol in the mobile phase hence decreases its adsorption energy onto the stationary phase. Second, increasing the temperature increases the mobility of the alkyl chains bonded to the surface and these chains become more "liquid-like". The isotherm parameters derived earlier in this work show that increasing the temperature decreases the number of low-energy sites accessible to phenol (q_{s1}, Fig. 5a) but does not affect the number of high-energy sites accessed by phenol (q_{s2}, Fig. 5c). The low-energy sites have been related to the alkyl chains bonded to the silica surface, chains with which the solute interacts by weak hydrophobic interactions [8]. Increasing the mobility of the bonded chains seems to decrease the accessible contact area between the alkyl chains and the solution, possibly due to their increased mobility. In contrast, the lack of influence of the temperature on q_{s2} suggests that the increased mobility of the chains has no influence on the high-energy sites accessed by phenol. This is consistent with the association of these sites with cavities residing deep inside the bonded layer of alkyl chains [16]. The increased mobility of the chains with increasing temperature would have little

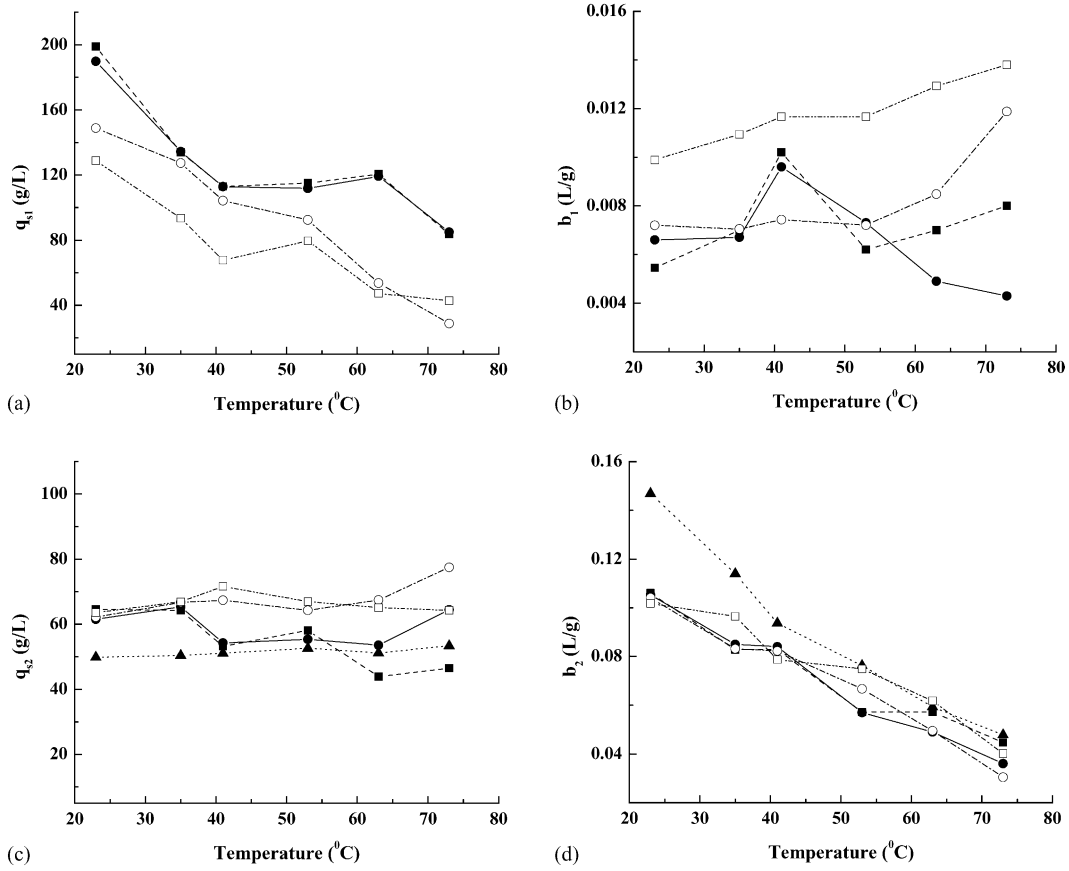

Fig. 5. Influence of the temperature on: (a) the saturation capacity of the low-energy sites (q_{s1}), (b) the adsorption constant of the low-energy sites (b_1), (c) the saturation capacity of the high-energy sites (q_{s2}), and (d) the adsorption constant of the high-energy sites (b_2). Each subfigure shows the corresponding isotherm parameter calculated by: non-linear fitting of the isotherm data to the bi-Langmuir isotherm model (●), affinity energy distribution (■), the inverse method, using overloaded band profiles obtained by injecting: 10 g/L phenol solution for 40 s (▲), 50 g/L phenol solution for 40 s (◯), and 100 g/L phenol solution for 40 s (□).

influence on the number of high-energy sites accessible by phenol, since this number depends mostly on the fluctuations of the local density of silicon atoms of the silica surface that are bonded to alkyl chains.

The isotherm parameters derived earlier in this work also show that increasing the temperature causes a slight increase of the adsorption constant of the low-energy sites (b_1, Fig. 5b) and a rapid decrease of the adsorption constant of the high-energy sites (b_2, Fig. 5d). The slight increase of b_1 with increasing temperature might be due to the mobility of the chains increasing with increasing temperature and causing a decrease of the entropy cost due to the insertion of the solute molecules between the partially ordered chains. The decrease of b_2 with increasing temperature is mostly a consequence of the correlative increase of the solubility of phenol in the mobile phase, combined with a slow decrease of the adsorption energy on the high-energy sites (Fig. 6). As in the case of the low-energy sites, the increased mobility of the chains at higher temperature should cause a decrease of the entropy cost. However, the high-energy sites reside deep within the chains, where the chains are more rigid than their free extremities close to the surface of the stationary phase, which limits the consequences of this increased mobility.

The low-energy sites on alkyl-bonded silica stationary phases have been assimilated to those sites with which phenol molecules have only weak, non-polar, hydrophobic interactions while the high-energy sites have been related to those sites where unreacted silanol groups can interact strongly with phenol molecules by polar interactions. Fig. 6 shows plots of the difference between the mean adsorption energies on the high- and the low-energy sites, calculated using the following equation:

$$\varepsilon_{a,2} - \varepsilon_{a,1} = RT \ln\left(\frac{b_2}{b_1}\right) \quad (13)$$

under the assumption that the pre-exponential factor is the same for all the sites on the stationary phase [8]. The difference between the adsorption energies on the two sites decreases with increasing temperature, approximately from 7 kJ/mol at 23 °C to 2.5 kJ/mol at 73 °C. The difference is less than 10 kJ/mol at all the temperatures studied. This value is too small to be consistent with the involvement of interactions between phenol molecules

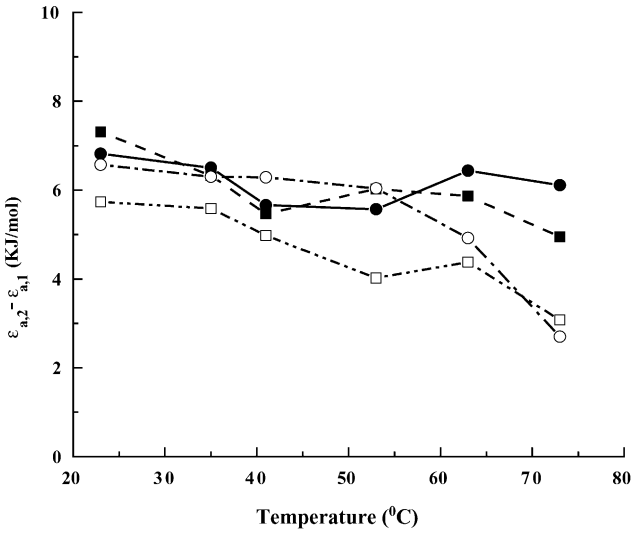

Fig. 6. Difference between the adsorption energies of the high- and the low-energy sites vs. the temperature. The figure shows this energy difference calculated from the results of: non-linear fitting of the isotherm data to the bi-Langmuir isotherm model (●), affinity energy distribution (■), the inverse method, using overloaded band profiles obtained by injecting 50 g/L phenol solution for 40 s (◯), and 100 g/L phenol solution for 40 s (□).

and silanol groups in the adsorption on the high-energy sites.

In summary, the results from this study support the previous suggestion that the high-energy sites reside deep within the layer of alkyl chains while the low-energy sites reside on the surface of a dense network of chains [8,16].

5. Conclusion

The results of our investigation of the effect of the temperature on the isotherm parameters of phenol on Symmetry-C_{18} demonstrate the power of the method used. Frontal analysis data were acquired under a set of experimental conditions selected in the center of the range of interest. The modeling of these data was informed by the results of the AED calculations. Finally, the inverse method allowed the rapid determination of the numerical values of the parameters of the selected isotherm model, in the whole range of conditions that had to be investigated. The validity of the approach was demonstrated by the agreement between the numerical values afforded by the different methods for the isotherm coefficients.

In the case studied, the adsorption data follow bi-Langmuir isotherm behavior. Two of the four parameters of the isotherm, the adsorption constant on the low-energy sites and the saturation capacity of the high-energy sites, remain practically constant in the temperature range studied while the other two parameters, the adsorption constant on the high-energy sites and the saturation capacity of the low-energy sites decrease steadily with increasing temperature. Thus, the decrease of the retention time with increasing temperature that is observed in Fig. 3 results from the combination of the decrease of the saturation capacity of the low-energy sites and the decrease of the adsorption constant on the high-energy sites. These variations are consistent with the model of retention mechanism suggested earlier. The low-energy sites consist in the interface between the mobile phase and the exposed alkyl chains bound to the silica support while the high-energy sites consist in holes between the bonded chains. These holes are accessible to sufficiently small molecules like phenol and provide enhanced lateral interactions between the bonded ligands and the adsorbates.

These results cast serious doubts on the value of the thermodynamic information derived from the conventional Van't Hoff plots of the retention factors. These factors are proportional to the initial slope of the isotherm. They are the sum of the contributions of the different types of sites that exist on the adsorbent surfaces, surfaces that are always heterogeneous. As shown here, the temperature dependence of these contributions result from the different temperature dependence of the adsorption constants and the saturation capacities of the low- and the high-energy sites. Accordingly, the overall temperature dependence of retention factors are meaningless.

Similar conclusions were derived earlier from the study of the influence on the isotherm coefficients of the methanol concentration of the aqueous mobile phase [8,16]. Increasing this concentration caused a large decrease of the equilibrium constant on the high-energy sites and a much smaller decrease in that on the low-energy sites. Thus, for the low-energy sites, the decreased entropy cost due to the increased mobility of the bonded chains with increasing methanol concentration compensates the increased competition of methanol and the increased solubility of phenol in the mobile phase. In contrast, this compensation takes place to a much smaller extent for the high-energy sites. The saturation capacities of the two sites decrease both with increasing methanol concentration. In the case of the high-energy sites, this might be explained by a possible competition between methanol and phenol for access to the high-energy sites although the adsorption of methanol, even on the high-energy sites, is weak.

Our present results seem to confirm and reinforce the conclusions of this previous work. The surface of most alkyl-bonded silica seems to be heterogeneous. Two types of sites, both rather homogeneous, coexist on these surfaces. The low-energy sites seem to exist on the surface of the bonded chains. The high-energy sites consist in deep cavities within the alkyl layer, cavities that are accessible for sufficiently small molecules such as phenol. The small difference between the adsorption energies of the high- and the low-energy sites suggests that these two types of sites are of similar nature.

Acknowledgements

This work was supported in part by Grant CHE-02-44693 of the National Science Foundation and by the cooperative

agreement between the University of Tennessee and the Oak Ridge National Laboratory.

References

[1] H. Colin, G. Guiochon, J. Chromatogr. 141 (1977) 289.
[2] R.E. Majors, LC-GC Mag. 6 (1988) 298.
[3] W. Melander, Cs. Horváth, in: Cs. Horváth (Ed.), High Performance of Liquid Chromatography: Advances and Perspectives, vol. 2, Academic press, New York, 1980.
[4] J.G. Dorsey, K.A. Dill, Chem. Rev. 89 (1989) 331.
[5] A. Vailaya, Cs. Horváth, J. Chromatogr. A 829 (1998) 1.
[6] D.M. Bliesner, K.B. Sentell, J. Chromatogr. 631 (2003) 23.
[7] J.L. Wysocki, K.B. Sentell, Anal. Chem. 70 (1998) 602.
[8] F. Gritti, G. Guiochon, J. Chromatogr. A 995 (2003) 37.
[9] L.A. Cole, J.G. Dorsey, Anal. Chem. 64 (1992) 1317.
[10] K. Miyabe, G. Guiochon, Anal. Chem. 74 (2002) 5982.
[11] C.A. Doyle, T.J. Vickers, C.K. Mann, J.G. Dorsey, J. Chromatogr. A 877 (2000) 41.
[12] M.W. Ducey, C.J. Orendorff, J.E. Pemberton, L.C. Sander, Anal. Chem. 74 (2002) 5576.
[13] W.R. Melander, B.K. Chen, Cs. Horváth, J. Chromatogr. 318 (1985) 1.
[14] M. Gorgenyi, K. Heberger, J. Chromatogr. A 985 (2003) 11.
[15] K. Jinno, T. Nagoshi, N. Tanaka, M. Okamoto, J.C. Fetzer, W.R. Biggs, J. Chromatogr. 436 (1988) 1.
[16] F. Gritti, G. Guiochon, Anal. Chem. 75 (2003) 5726.
[17] M. Jaroniec, R. Madey, Physical Adsorption on Heterogeneous Solids, Elsevier, New York, 1988.
[18] A. Larsson, Mol. Immunol. 25 (1988) 1239.
[19] H. Ardebrant, R.J. Pugh, Colloids Surf. 53 (1991) 101.
[20] J.V. Selinger, S.Y. Rabbany, Anal. Chem. 69 (1997) 170.
[21] R.J. Umpleby, C.B. Sarah, C. Yizhao, N.S. Ripal, K.D. Shimizu, Anal. Chem. 73 (2001) 4584.
[22] B.J. Stanley, G. Guiochon, J. Phys. Chem. 97 (1993) 8098.
[23] M. Pyda, B.J. Stanley, M. Xie, G. Guiochon, Langmuir 10 (1994) 1573.
[24] B.J. Stanley, G. Guiochon, Langmuir 10 (1994) 4278.
[25] B.J. Stanley, G. Guiochon, Langmuir 11 (1995) 1735.
[26] B.J. Stanley, J. Krance, J. Chromatogr. A 1011 (2003) 11.
[27] G. Gotmar, D. Zhou, B.J. Stanley, G. Guiochon, Anal. Chem. 76 (2004) 197.
[28] B.J. Stanley, P. Szabelski, Y.-B. Chen, B. Sellergren, G. Guiochon, Langmuir 19 (2003) 772.
[29] A. Felinger, D. Zhou, G. Guiochon, J. Chromatogr. A 1003 (2003) 73.
[30] F. Gritti, G. Guiochon, J. Chromatogr. A 1033 (2004) 43.
[31] M. Kele, G. Guiochon, J. Chromatogr. A 830 (1999) 55.
[32] I. Quinones, G. Guiochon, J. Chromatogr. A 796 (1998) 15.